



ELSEVIER

Theoretical and Applied Fracture Mechanics 30 (1998) 153–158

theoretical and
applied fracture
mechanics

Material instability criterion near a notch-tip under locally adiabatic deformations of thermoviscoplastic materials

L. Chen, R.C. Batra *

Department of Engineering Science and Mechanics, MC 0219, Virginia Polytechnic Institute and State University, Blacksburg, VA 24061, USA

Abstract

A material instability criterion for locally adiabatic plane strain deformations of a thermoviscoplastic material near a notch-tip is proposed. It is used to rank eight materials according to their susceptibility to instability. © 1998 Elsevier Science Ltd. All rights reserved.

1. Introduction

Locally adiabatic torsional deformations of a thin-walled tube whose thickness varied sinusoidally in the axial direction and the thickness at the midsection equalled 90% of that at the edges have been numerically simulated in [1]. The thermoviscoplastic response of the material of the tube was modeled by the relation proposed in [2], and the torque required to twist the tube was computed. By comparing the nominal shear strain at which the torque rapidly dropped, 12 materials were ranked according to their susceptibility to adiabatic shear banding. The torsion test has been used [3] to experimentally study the initiation, growth and propagation of a shear band. In the torsion test involving a thick-walled tube with a v-notch around its circumference, a shear band usually propagates in a direction perpendicular to the particle velocity. Thus if a shear band is viewed

as a crack, the state of deformation in the language of the linear elastic fracture mechanics corresponds to Mode III. In the torsion of a thin-walled tubular specimen, a shear band initiating at a point usually propagates in the direction of the particle velocity and it corresponds to Mode II deformations. The initiation, growth and propagation of a shear band from the notch tip in a prenotched plate impacted on the side by a cylindrical projectile moving parallel to the axis of the notch, have been experimentally studied in [4–6]. The crack-tip deformation field is predominantly Mode II, i.e., in-plane shearing.

In a previous investigation on the direction of instability in an impact loaded prenotched plate, it was assumed that the material is elastic/perfectly-plastic, HRR-type singular fields exist near the notch-tip, and an instability initiates in the direction of the maximum effective plastic strain. The direction of instability was found to be close to that observed experimentally. In this article, an instability criterion for locally adiabatic deformation near a crack-tip is proposed. This criterion suggests that the Mode-II stress intensity factor

*Corresponding author. Tel.: +1 540 231 6051; fax: +1 540 231 4574; e-mail: rbatra@vt.edu.

can be used to rank thermoviscoplastic materials according to their susceptibility to the onset of instability at a crack-tip in locally adiabatic high strain-rate deformations. The delay between the initiation of a shear band and the onset of material instability depends upon the thermal-softening and strain and strain-rate hardening characteristics of the material, the loading conditions, and the shapes, sizes and number of defects present in the body.

2. An instability criterion

It has been reported [5] that soon after a pre-notched plate is impacted by a projectile moving parallel to the axis of the notch, fringe patterns around the crack tip exhibit deformation characteristics of a Mode II plastic zone evolving under small scale yielding conditions. Let a viscoplastic zone, P , develop around the crack tip, and the region outside of P deform elastically. The flow stress for the material in the viscoplastic zone, prior to the onset of adiabatic shear instability, is assumed to be given by the relation [2]:

$$\sigma_m = (A + B\gamma_p^n) \left(1 + C \ln \frac{\dot{\gamma}_p}{\dot{\gamma}_0} \right) (1 - T^{*m}), \quad (1)$$

where

$$T^* = \alpha(T - T_0), \quad \alpha = 1/(T_m - T_0), \quad (2)$$

and σ_m , γ_p , $\dot{\gamma}_p$, and T are the effective flow stress, the effective plastic strain, the effective plastic strain-rate and the temperature, respectively. Parameters A , B , C , n and m are characteristic of the material of the body, T_0 is the ambient temperature, T_m the melting temperature of the material, $\dot{\gamma}_0$ a reference strain rate and A equals the yield stress in a quasistatic simple tension or compression test. Different constitutive relations [7] between γ_p , $\dot{\gamma}_p$, σ_m and T have been found to give essentially similar results for the initiation and growth of shear bands in a thermoviscoplastic body deformed in simple shear. Here relation (1) with $m = 1.0$ is used mainly because values of parameters A , B , etc. are available for several materials. Test data given in [8] suggests that the flow stress is an affine function of the temperature rise.

An instability criterion first for general 3-dimensional deformations and then for plane strain deformations near a crack-tip is derived. It is assumed that the deformations in the viscoplastic zone are locally adiabatic. Numerical experiments [9] have shown that heat conduction has negligible effect on the value of the effective plastic strain at the instant of the initiation of a shear band. The balance of internal energy with heat conduction neglected can be written as

$$\rho c_v dT = \beta \sigma_m d\gamma_p, \quad (3)$$

where ρ is the mass density, c_v the specific heat, and $\beta \approx 0.9$ the Taylor–Quinney constant that equals the fraction of the viscoplastic work converted into heat.

It is postulated in [10] that a material point becomes unstable when σ_m attains a maximum value. Experiments [3] on high strain-rate torsion of thin-walled steel tubes and their numerical simulations (e.g. see [13]) reveal that a shear band initiates at a value of the effective plastic strain much larger than that corresponding to the maximum value of σ_m . The instability condition

$$\frac{d\sigma_m}{d\gamma_p} = 0, \quad (4)$$

and Eq. (3) give

$$\frac{\partial \sigma_m}{\partial \gamma_p} + \frac{\partial \sigma_m}{\partial \dot{\gamma}_p} \frac{d\dot{\gamma}_p}{d\gamma_p} + \frac{\partial \sigma_m}{\partial T} \frac{\beta \sigma_m}{\rho c_v} = 0. \quad (5)$$

Substitution from Eq. (1) into Eq. (5) and a rearrangement of the terms yields

$$\frac{dg}{d\gamma_i} = -Bn\gamma_i^{n-1} \frac{g}{A + B\gamma_i^n} + \frac{\alpha\beta}{\rho c_v} (A + B\gamma_i^n) g^2, \quad (6)$$

where $g = (1 + C \ln(\dot{\gamma}_i/\dot{\gamma}_0))$, and γ_i and $\dot{\gamma}_i$ equal, respectively, the effective plastic strain and the effective plastic strain-rate at the onset of material instability. An integral of Bernoulli's ordinary differential Eq. (6) gives

$$\left(1 + C \ln \frac{\dot{\gamma}_i}{\dot{\gamma}_0} \right) \left(\frac{A}{B} + (\gamma_i)^n \right) \left(D - \frac{\alpha\beta B}{\rho c_v} \gamma_i \right) = 1, \quad (7)$$

where D is a constant of integration. In order for Eq. (7) to hold, D must be positive and

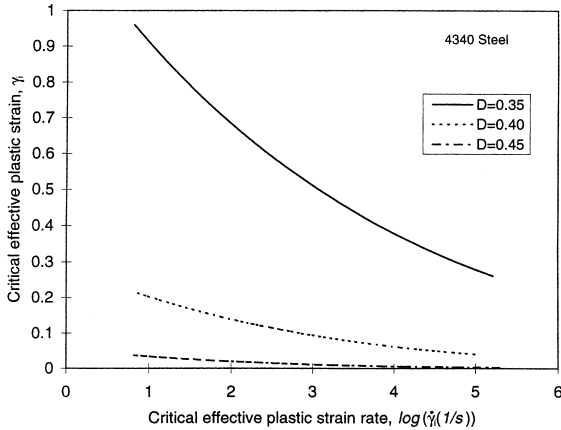


Fig. 1. A relationship between the effective plastic strain-rate and the effective plastic strain corresponding to the onset of material instability in a 4340 steel for three different values of the constant of integration, D .

$\gamma_i < D\rho c_v/\alpha\beta B$. In [11] D was found to be 1.1536 for a titanium alloy for which $A=465$ MPa, $B=530$ MPa, $n=1$, $C=0.0245$, $\dot{\gamma}_0 = 2.1 \times 10^{-3}/s$, $\alpha = 0.00137/K$, $\rho = 7800$ kg/m³, $c_v = 527$ J/kg K. Fig. 1 depicts the relationship between γ_i and $\dot{\gamma}_i$ for the 4340 steel with values of material parameters listed in Table 1, and for $D=0.35, 0.40$ and 0.45 . Note that the relationship between γ_i and $\dot{\gamma}_i$ is very sensitive to the value of D . Recalling that $d\gamma_i/d\dot{\gamma}_i = (d\gamma_i/d \log \dot{\gamma}_i)/\dot{\gamma}_i$, one can see that for $\dot{\gamma}_i < 10^3/s$, the effective plastic strain decreases rapidly with an increase in the effective plastic strain-rate. However, for $\dot{\gamma}_i \geq 10^3/s$, the rate of change of γ_i with respect to $\dot{\gamma}_i$ is negligibly small.

Since adiabatic shear bands form during high strain-rate deformations of a thermoviscoplastic body, it is assumed henceforth that the effective

plastic strain-rate is constant and equals $\dot{\gamma}_*$. Then Eqs. (1) and (3) give

$$\sigma_m = (A + B(\gamma_p)^n)(1 + C \ln(\dot{\gamma}_*/\dot{\gamma}_0)) \times \exp \left[-\frac{\alpha\beta}{\rho c_v} (1 + C \ln(\dot{\gamma}_*/\dot{\gamma}_0))(A\gamma_p + B\gamma_p^{n+1}/(n+1)) \right] \quad (8)$$

which when combined with Eq. (4) gives

$$\frac{\gamma_i^{n-1}}{(A + B\gamma_i^n)^2} = \frac{\alpha\beta}{n\rho Bc_v} (1 + C \ln(\dot{\gamma}_*/\dot{\gamma}_0)), \quad (9)$$

where γ_i is the effective plastic strain at which σ_m is maximum; below it is called the critical effective plastic strain or the shear instability strain.

For a power law strain-hardening material, $A=0$ and B is proportional to the initial yield stress of the material at a strain-rate of $\dot{\gamma}_0$. In this case, Eq. (9) gives

$$\gamma_i = \left(\frac{n\rho c_v}{\bar{B}\alpha\beta} \right)^{1/(n+1)}, \quad (10)$$

where $\bar{B} = B(1 + C \ln(\dot{\gamma}_*/\dot{\gamma}_0))$ is proportional to the initial yield stress of the material at a strain-rate of $\dot{\gamma}_*$.

For all eight materials listed in Table 1, the strain-hardening exponent $n < 1$. Therefore, either from Eq. (9) or from Eq. (10), it follows that

$$\frac{d\gamma_i}{d\dot{\gamma}_*} < 0. \quad (11)$$

That is, the shear instability strain γ_i decreases with an increase in the effective plastic strain-rate $\dot{\gamma}_*$. For $\dot{\gamma}_* = 10^5/s$, values of the shear instability strain γ_i , computed from Eq. (9) for the eight

Table 1
Material constants from [12] for the constitutive relation (1) ($\dot{\gamma}_0 = 10^{-3}/s$, $T_0 = 25^\circ C$)

Material	A (MPa)	B (MPa)	C	n	m	ρ (kg/m ³)	T_m (°C)	K (GPa)	μ (GPa)	c_v (J/kg°C)
OFHC Copper	89.63	291.64	0.025	0.31	1.09	8960	1083	138	42	383
1006 Steel	350.25	275.00	0.022	0.36	1.00	7890	1538	169	80	452
2024 T351 Aluminum	264.75	426.09	0.015	0.34	1.00	2770	502	76	28	875
7039 Aluminum	336.46	342.66	0.01	0.41	1.00	2770	604	81	28	875
4340 Steel	792.19	509.51	0.014	0.26	1.03	7840	1520	157	76	477
S-7 Tool Steel	1538.89	476.42	0.012	0.18	1.00	7750	1490	246	117	477
Tungsten	1505.79	176.50	0.016	0.12	1.00	17000	1450	257	133	134
Depleted Uranium	1079.01	1119.69	0.007	0.25	1.00	18600	1200	92	58	117

Table 2

Instability strain, shear band initiation strain, effective strain at the initiation of a shear band in the torsion test, and critical stress, $(\sigma_{II})_i$, for eight materials

Material	Instability strain at $10^5/s$ strain-rate	Strain at $10^5/s$ strain rate when		Effective strain at the initiation of a shear band in a torsion test	Critical stress (GPa) at $10^5/s$ strain-rate
		$\sigma_{\text{eff}} = 0.9\sigma_{\text{max}}$	$\sigma_{\text{eff}} = 0.8\sigma_{\text{max}}$		
OFHC Copper	1.587	3.259	4.224	3.65	22
1006 Steel	1.086	2.731	3.722	1.5	18
2024 T351 Aluminum	0.322	0.768	1.035	0.7	9.6
7039 Aluminum	0.387	0.965	1.309	1.08	12
4340 Steel	0.358	1.224	1.803	1.60	11
S-7 Tool Steel	0.0793	0.514	0.860	0.2	4.8
Tungsten	0.0136	0.237	0.447	0.14	2.1
Depleted Uranium	0.13	0.441	0.641	0.16	6.3

materials with material parameters given in Table 1, are listed in Table 2. Based on numerical simulation of shear bands in simple shearing problems for 12 materials, it was postulated in [13] that a shear band initiates in earnest when the effective stress has dropped to 90% of its peak value. However, in [14], a shear band was assumed to initiate when the effective stress has dropped to 80% of its peak value. Values of the effective plastic strain, γ_s , at which a shear band will initiate according to these two hypotheses are listed in Table 2. One reason for the large differences between the corresponding values in columns 3 and 5 is that the values in column 5 strongly depend upon the defect shape and size. The instability strain listed in column 2 and the computed strains in columns 3 and 4 are material properties, but the value of the effective strain given in column 5 depends upon the material, shape of the structure, loading conditions and the defect shape and size. For a large enough defect, a shear band may initiate even before the effective stress attains its peak value; e.g. see [15].

The aforestated result (9) is now used to obtain an instability criterion near a notch-tip. For plane strain deformations of an elastic-plastic material, the following expression for the effective plastic strain near the notch-tip was derived in [16].

$$\gamma_p = \left(\frac{K_{II}^2}{2\sigma_0 \pi r E} \right) \gamma_{pl}(m^e, \theta). \quad (12)$$

Here K_{II} is the Mode-II stress intensity factor, σ_0 the yield stress of the elastic-perfectly plastic material,

$$m^e = \frac{2}{\pi} \tan^{-1} \left(\frac{K_I}{K_{II}} \right),$$

the mode mixity parameter, K_I the Mode-I stress intensity factor, E Young's modulus, and (r, θ) cylindrical coordinates of a point with the origin at the notch-tip. The expression for γ_{pl} in terms of the far-field solution is given in [16] where it is also stated that the nonlinear equations

$$\frac{\partial \gamma_p}{\partial K_I} = 0, \quad \frac{\partial \gamma_p}{\partial K_{II}} = 0, \quad \frac{\partial \gamma_p}{\partial \theta} = 0, \quad (13)$$

may not have a solution for K_I , K_{II} and θ which maximizes γ_p . For Kalthoff's experiment, it was found in [17] that for the time interval of interest, the mode mixity parameter m^e is essentially constant. For a fixed value of m^e , conditions

$$\frac{\partial \gamma_{pl}}{\partial \theta}(m^e, \theta) = 0, \quad \frac{\partial^2 \gamma_{pl}(m^e, \theta)}{\partial \theta^2} < 0, \quad (14)$$

are solved to obtain $\theta_i = \theta_i(m^e)$ which makes γ_p maximum.

Eq. (12) is now postulated to be approximately valid for locally adiabatic deformations of a thermoviscoplastic material till the onset of material instability. This assumption is reasonable for several materials since the temperature rise until this point is not much because of the rather small plastic deformations of the body. Eqs. (9), (12) and (14) yield

$$(\sigma_{II})_i \equiv \frac{(K_{II})_i}{\sqrt{r_i}} = \left[\frac{2\pi E \sigma_0}{\gamma_{pl}(m^e, \theta_i)} \gamma_i(\dot{\gamma}_*) \right]^{1/2}. \quad (15)$$

Here $r_i > 0$ is the distance from the notch tip of the point where a material instability initiates. Experimental observations in [18] indicate that $r_i = 0.8 \mu\text{m}$, and finite element simulations [19] exhibit that $r_i > 0$. In general, the value of r_i will depend upon the material of the plate and the notch-tip radius. It is hypothesized that $(\sigma_{II})_i$ is a measure of the material's susceptibility to adiabatic shear instability near a notch-tip in locally adiabatic plane strain deformations of a thermoviscoplastic body. Thus, the Mode II stress-intensity factor determines material's susceptibility to the onset of a shear instability at a crack-tip in plane strain deformations.

The adiabatic shear localization phenomenon during the axisymmetric punching of a hole in a plate supported on a die has been experimentally studied in [20]. Shear bands were found to initiate at points on the boundaries of the punch/plate and die/plate interfaces in a 4340 steel plate when the Mode-II stress intensity factor there equalled $210 \text{ MPa} \sqrt{m}$. The length of the process zone near the notch-tip in a prenotched plate under impact loading was found to equal the radius, $75 \mu\text{m}$, of the notch tip. It suggests that r_i in Eq. (15) is atmost equal to the notch-tip radius. Knowing $(K_{II})_i$, Eq. (15) can be used to evaluate r_i , the distance from the notch-tip where a material instability initiates.

Values of the critical Mode II stress, $(\sigma_{II})_i$, for the eight materials listed in Table 1 and characterized by affine thermal softening are listed in Table 2. In computing these values, $\dot{\gamma}_*$ was set

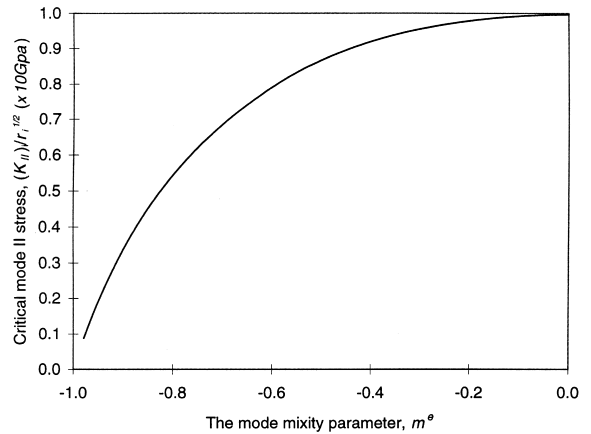


Fig. 3. Dependence of the critical stress, $(\sigma_{II})_i$, upon the mode-mixity parameter, m^e , for the 4340 steel at $\dot{\gamma}_* = 10^5/\text{s}$.

equal to $10^5/\text{s}$, and $m^e = -0.21$. For $m^e = -0.21$, the critical instability angle is computed to be -13° for the OFHC copper, and -12° for the other seven materials. The dependence of the critical Mode-II stress on the effective plastic strain rate, $\dot{\gamma}_*$ is plotted in Fig. 2 for the 4340 steel and for $m^e = -0.11, -0.21$ and -0.37 . These plots reveal that the qualitative nature of the curves remains unaffected by the value of m^e . Fig. 3 exhibits the dependence of $(\sigma_{II})_i$ upon m^e for the 4340 steel and $\dot{\gamma}_* = 10^5/\text{s}$. The value of $(\sigma_{II})_i$ increases by a factor of 10 when m^e is increased from -0.98 to 0. Numerical experiments show that the mode mixity

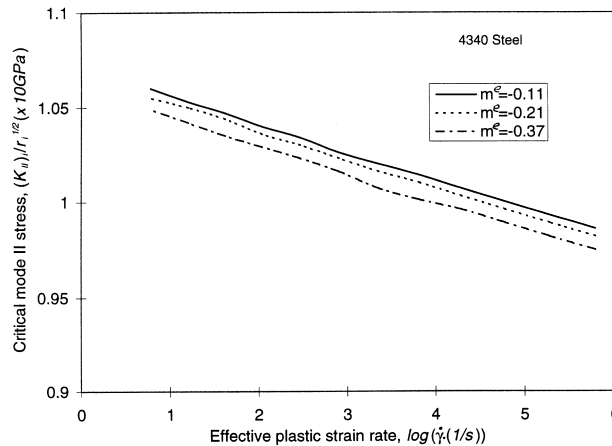


Fig. 2. Dependence of the critical stress, $(\sigma_{II})_i$, upon the effective plastic strain-rate for the 4340 steel for three different values of m^e .

parameter does not affect the ranking of these eight materials, and an increase in the effective plastic strain rate decreases by a small amount the critical stress, $(\sigma_{II})_i$. The computed values of $(\sigma_{II})_i$ suggest that the material instability at a crack-tip will initiate in the following order in plane strain deformations of these eight materials: Tungsten, S-7 Tool Steel, Depleted Uranium, 2024-T351 Aluminum, 4340 Steel, 7039 Aluminum, 1006 Steel, OFHC Copper.

3. Conclusions

A material instability criterion for plane strain deformations near a notch-tip in a plate made of a thermoviscoplastic material has been proposed. It elucidates that the Mode-II stress intensity factor at the notch-tip is a determining factor in material's susceptibility to shear instability. Eight materials have been ranked according to their susceptibility to material instability at a notch-tip and this ranking essentially agrees with that obtained earlier based on the numerical simulation of torsion of thin-walled tubular specimens.

Acknowledgements

This work was supported by the ONR grant N00014-98-1-0300 with Dr. Y.D.S. Rajapakse as the program manager.

References

- [1] R.C. Batra, X. Zhang, T.W. Wright, Critical strain ranking of 12 materials in deformations involving adiabatic shear bands, *J. Appl. Mech.* 62 (1995) 252–255.
- [2] G.R. Johnson, W.H. Cook, A constitutive model and data for metals subjected to large strain rates and high temperatures, *Proceedings of the Seventh International Symposium on Ballistics*, The Hague, The Netherlands, 1983, pp. 541–548.
- [3] A. Marchand, J. Duffy, An experimental study of the formation process of adiabatic shear bands in a structural steel, *J. Mech. Phys. Solids* 36 (1988) 251–283.
- [4] J.F. Kalthoff, S. Winkler, Failure mode transition at high strain rates of loading, in: C.Y. Chiem, H.D. Kunze, L.W. Meyer (Eds.), *Proceedings of the International Conference on Impact Loading and Dynamic Behavior of Materials*, Deutsche Gesellschaft für Metallkunde, DGM, Bremen, 1988, pp. 185–196.
- [5] J.J. Mason, A.J. Rosakis, G. Ravichandran, Full field measurements of the dynamic deformation field around a growing adiabatic shear band at the tip of a dynamically loaded crack or notch, *J. Mech. Phys. Solids* 42 (1994) 1679–1697.
- [6] M. Zhou, A.J. Rosakis, G. Ravichandran, Dynamically propagating shear bands in impact-loaded prenotched plates-I. Experimental investigations of temperature signatures and propagation speed, *J. Mech. Phys. Solids* 44 (1996) 981–1006.
- [7] R.C. Batra, C.H. Kim, Effect of viscoplastic flow rules on the initiation and growth of shear bands at high strain rates, *J. Mech. Phys. Solids* 38 (1990) 859–874.
- [8] J.F. Bell, *The physics of large deformation of crystalline solids*, Springer Tracts in Natural Philosophy, Springer, Berlin, 1968.
- [9] R.C. Batra, C.H. Kim, Effect of thermal conductivity on the initiation, growth, and band width of adiabatic shear bands, *Int. J. Eng. Sci.* 29 (1991) 949–960.
- [10] C. Zener, J.H. Hollomon, Effect of strain rate upon plastic flow of steel, *J. Appl. Phys.* 15 (1944) 22–32.
- [11] L.L. Wang, A criterion of thermoviscoplastic instability for adiabatic shearing, *Proceedings of the First International Symposium on Intense Dynamic Loading*, Science Press, Beijing, 1986, pp. 787–792.
- [12] A.M. Rajendran, High strain rate behavior of metals, ceramics and concrete, Report #WL-TR-92-4006, Wright Patterson Air Force Base, 1992.
- [13] R.C. Batra, C.H. Kim, Analysis of shear banding in twelve materials, *Int. J. Plasticity* 8 (1992) 425–452.
- [14] B. Deltort, Experimental and numerical aspects of adiabatic shear in a 4340 steel, *J. de Physique C* 8 (4) (1994) 447–459.
- [15] R.C. Batra, The initiation and growth of, and the interaction among, adiabatic shear bands in simple and dipolar materials, *Int. J. Plasticity* 3 (1987) 75–89.
- [16] L. Chen, R.C. Batra, Analysis of material instability at an impact loaded crack tip, *Theoretical and Appl. Fract. Mech.* 29 (1998) 213–217.
- [17] Y.J. Lee, L.B. Freund, Fracture initiation due to asymmetric impact loading of an edge cracked plate, *J. Appl. Mech.* 57 (1990) 104–111.
- [18] L. Wang, X. Dong, S. Hu, J. Yu, A macro- and microscopic study of adiabatic shearing extension of mode-II crack at dynamic loading, *J. de Physique IV* 4 (1994) 465–470.
- [19] J. Faleskog, Effects of local constraints along three-dimensional crack fronts – a numerical and experimental investigation, *J. Mech. Phys. Solids* 43 (1995) 447–493.
- [20] K.M. Roessig, J.J. Mason, Adiabatic shear localization in the impact of edge notched specimens, submitted for publication.